

## **Focused ion beam irradiation platform with a 3-D fluorescence imaging system: a flexible tool for cancer research**

Andrew D. Harken<sup>1,2</sup>, Naresh T. Deoli<sup>1,2</sup>, Citlali Perez Campos<sup>3</sup>, Brian Ponnaiya<sup>1,2</sup>, Guy Garty<sup>1,2</sup>, Grace S. Lee<sup>3</sup>, Malte J. Casper<sup>3</sup>, Shikhar Dhingra<sup>3</sup>, Gary W. Johnson<sup>2</sup>, Sally A. Amundson<sup>2</sup>, Peter W. Grabham<sup>2</sup>, Elizabeth M. C. Hillman<sup>3</sup>, and David J. Brenner<sup>1,2</sup>

1. *Radiological Research Accelerator Facility, Columbia University Irving Medical Center, 136 S. Broadway, P.O. Box 21, Irvington, New York 10533*
2. *Center for Radiological Research, Columbia University Irving Medical Center, 630 W. 168th Street, New York, NY 10032*
3. *Laboratory for Functional Optical Imaging, Departments of Biomedical Engineering and Radiology, Zuckerman Mind Brain Behavior Institute and Kavli Institute for Brain Sciences, Columbia University, New York, NY, 10027*

### **ABSTRACT**

To improve particle radiotherapy, we need a better understanding of the biology of targeted and non-targeted radiation effects. This is particularly important in the field of heavy ion radiation therapy where global effects are observed, yet only a subset of cells receive a high energy deposition from ion tracks. To allow real-time 3D imaging of living biological samples during and after irradiation with a focused ion beam, we have integrated a high-speed light sheet fluorescence imaging system (swept confocally aligned planar excitation, SCAPE microscopy) into the focused ion beam irradiation platform (FIBIP) at the Columbia University Radiological Research Accelerator Facility (RARAF). The RARAF FIBIP is centered on a 7 T superconducting solenoid magnet, which focuses an ion beam, generated by RARAF's ion accelerators, to a field size of between 5 mm and 2  $\mu$ m. An integrated SCAPE volumetric imaging system with associated environmental control allows sub-second observation of 3D cell cultures sample over extended periods before, during, and after radiation treatments. The developed system enables exploration of the mechanistic effects of ion radiotherapy at the cellular and tissue levels. Here, we report details of the integrated system, and show an example of intracellular calcium signaling following ionizing radiation in U87 human glioblastoma 3D cultures using the integrated system.

## Introduction

### *Background*

Over 50% of cancer patients are treated with radiation therapy (RT)<sup>1,2</sup>. Charged particles (protons and carbon ions) are a preferred choice for RT modalities due to their localized physical dose with minimal lateral scattering in surrounding healthy tissues<sup>3</sup>. Radiation types are usually characterized by their linear energy transfer (LET), i.e., the energy a particle deposits in the tissue along its path. Amongst charged particles, the radiation dose of high-LET ( $>10$  keV/ $\mu$ m) particles in the tumor is more concentrated around the ion track, compared to low-LET ( $<1$  keV/ $\mu$ m) particles, thus controlling toxicity of normal tissue<sup>4</sup>. There is now increasing clinical data on the success of particle RT in treating cancers that are typically refractive to conventional low-LET therapy, including cancers such as pancreas, rectum and sarcomas<sup>5</sup>. However, little is known about the underlying molecular mechanisms that lead to efficacy. There has been some discussion<sup>6-10</sup> that as well as producing local effects to the tumor, particle RT may induce long-range systemic anti-cancer effects involving the immune system, and that these responses may be responsible for the overall success of the modality.

Therefore, developing a comprehensive understanding of cancer's molecular and cellular basis by identifying how tumors evolve, and how cells in the tumors respond to ionizing radiation is critical for radiation oncology. To achieve this goal, researchers need a combination of state-of-the-art tools that can deliver ionizing radiation to living cells in 3D cultures at clinically-relevant doses while simultaneously performing high-speed, functional time-lapse imaging at cellular resolution.

### *Swept confocally-aligned planar excitation (SCAPE) microscopy*

Cellular properties ranging from cell shape, to motility and mobility can provide read-out of cellular health and function. Fluorescent ion indicators and genetically-encoded fluorescent proteins can also permit optical assessment of cell signaling dynamics. Confocal microscopy has been widely used by biologists to investigate cellular structure dynamics, while two-photon microscopy is a popular tool for capturing calcium activity of neurons in the brain<sup>11</sup>. However, point-scanning microscopy methods such as these have limited volumetric imaging speeds and can also cause associated photodamage in sensitive samples. Light sheet microscopy can enable high-speed volumetric imaging of 3D tissues while also providing low phototoxicity<sup>12,13,14</sup>. Among the

different methods for light sheet microscopy, swept confocally-aligned planar excitation (SCAPE) microscopy has a valuable single-objective geometry, which leaves the other side of the sample unobstructed, permitting integration with sample perturbations<sup>13</sup> such as radiation. SCAPE also offers flexibility to image from 100 volumes-per-second to longitudinal time lapse imaging over hours<sup>15,16</sup>. SCAPE's compact and relatively simple design made it possible to integrate the system into our vertical microbeam.

### *Microbeam*

Charged particle microbeams are an excellent radiological research tool for delivering controlled doses to individual cells and for localizing the dose within a cell<sup>17</sup>. Our Radiological Research Accelerator Facility<sup>18</sup> (RARAF) is one of only a handful of ion microbeam facilities worldwide that is equipped for radiobiological research. While most of these facilities can target a specific cell or a region in the cell, translating from micrometer radiation delivery to mm radiation delivery with similar dose deposition is not available. The irradiation platform described here has been designed to deliver a range of beam sizes depending on experimental need, while its vertical configuration also permits biological sample dishes are placed horizontally for irradiation and imaging.

### *Environmental control*

The ability to particle microbeam irradiate *in vitro* 3D tissue models, which recapitulate disease and tissue processes better than cellular monolayers<sup>19</sup>, will advance our understanding of the role of cell signaling and tissue remodeling in radiation response<sup>20</sup>. However, it is imperative to preserve cells in 3D tissue in a viable state for long-term experiments ( $\geq 2$  h). This in turn requires maintenance of a controlled culture environment (37 °C; 5% CO<sub>2</sub>; and >97% relative humidity)<sup>21</sup>. Despite their small form factor, commercially-available benchtop cell culture environmental chambers cannot be practically accommodated in a vertical microbeam system<sup>15</sup>. Therefore, it was crucial to design a custom environmental control system around the vertical microbeam system, which not only allows the maintenance of cultures outside an incubator over an extended period, but also permits integration of the vertical microbeam system with a high-resolution and high-speed cellular imaging technique.

## *Summary*

By integrating our versatile superconducting solenoid-based vertical ion microbeam system with a fast light sheet microscopy and environmental control, we can now perform high-speed time-lapse imaging of live 3D cultures at cellular resolution during irradiation. We demonstrate this novel tool to capture the effect of acute irradiation with proton ions on the human U87 glioblastoma cell line grown in a 3D gel matrix. Specifically, the SCAPE imaging modality allowed us to monitor calcium signaling in U87 cells in a 3D gel matrix during treatment with 9 Gy of protons.

## **Methods**

### *Volumetric light sheet microscopy with SCAPE*

SCAPE microscopy is a high-speed 3D imaging method developed at the Columbia Laboratory for Functional Optical Imaging<sup>13,14</sup>. SCAPE captures 3D images by illuminating samples using a laterally swept oblique light sheet. The system incorporated into the linear accelerator followed the design of system D<sub>Z</sub> in Voleti et al<sup>14</sup> with modifications to include both 488 and 561 nm excitation and to facilitate objective positioning (see **Figure 1**).

Briefly, SCAPE passes merged 488 and 561 nm laser light (Coherent® OBIS™ lasers (488 nm and 561 nm) through a combination of a Powell and cylindrical lenses, which is then reflected off a galvanometer mirror via a long-pass dichroic, through a telescope that is focused towards the edge of the back focal plane of O1 a primary 1.0 NA 20x water immersion objective lens (Olympus, XLUMPLFLN20XW). This beam path forms an obliquely angled light sheet at the sample. Fluorescent light emitted from the sample is collected through the same objective lens, and passes back through the optical path, reflecting off the galvanometer mirror and passing through the dichroic into an additional telescope to reach the back of an air objective (O2 = Nikon CFI Plan Apo Lambda 20x/0.75 NA). With a magnification of 1.33 between O1 and O2 (corresponding to the ratio of the refractive index of water and air) this second objective forms a 3D oblique image of the illuminated plane at the sample. A third objective lens (O3 = Nikon CFI Plan Apo Lambda 10x/0.45 NA) is positioned obliquely such that its focal plane aligns with the oblique plane image. Note, for baseline tests without irradiation, measurements of cellular motility were acquired using an offline SCAPE system with O1, O2 and O3 all water-coupled Olympus,

XLUMPLFLN20XW). Light received into O3 is then passed through a dual color image splitter and focused using a 70 mm tube lens onto a high-speed sCMOS camera (Andor Zyla 4.2+). The image on the camera corresponds to an oblique optical section of the sample, where the focal plane of the camera is aligned with the plane illuminated by the oblique light sheet<sup>22</sup>.

High speed 3D images are acquired by moving the system's galvanometer mirror from side to side. This scanning changes the angle of the beam entering the back of O1, translating the oblique light sheet from side to side. Light coming from the sample is descanned by the same galvanometer mirror, in a similar way to a confocal microscope, causing the oblique light sheet image between O2 and O3 to remain stationary and thus continually focused on the camera. A full volume can thus be acquired by a single sweep of the galvo mirror, with images on the camera corresponding to focused images of the oblique light sheet as it sweeps laterally across the sample. This mechanism permits very efficient collection of optical sections at high speeds. The camera can read 100 rows (corresponding to 100 depths) at over 2000 frames per second, such that an image spanning 200 lateral steps can be acquired at 10 volumes-per-second. 3D images are acquired using only one moving part (the galvanometer moving at the volume rate), while the sample and primary objective lens remain stationary. Dual color data was collected simultaneously with both lasers on, using an image splitter (splitting at 560 nm) between O3 and the camera tube lens. Split green and red images were placed side by side onto the camera chip such that no additional rows needed to be acquired, thus maintaining the highest possible speed of imaging.

The single-objective nature of the SCAPE system enables samples to be imaged from above while the irradiation beam snout can access the sample from below. The simplicity of SCAPE's optical design made it compatible with proximity to the magnetic environment of the RARAF FIBIP, while its compact form factor permitted mounting of the entire microscope above the beam line. However, modifications to the ion beam focusing system were also required to expand the ion beam and ensure that ions could accurately reach the sample dish as detailed further below.

#### *Optimizing ion beam focusing within the irradiation platform*

Columbia University's RARAF facility has been designing, developing, and using focused ion beams for biological irradiation for more than 30 years<sup>17,23-35</sup>. The focusing systems have used

quadrupole focusing elements in electrostatic triplets and quadruplets<sup>24,33</sup> and permanent magnets<sup>26</sup>. We recently upgraded our ion focusing system to a 7 T superconducting solenoid (Cryomagnetics Inc, Oak Ridge, TN), designed to enable focusing of a wide range of particles (5 MeV H<sup>+</sup> to 30 MeV C<sup>6+</sup>) to spot sizes ranging from 5 mm down to 2  $\mu$ m in diameter. Our Focused Ion Beam Irradiation Platform (FIBIP) is centered on this new focusing modality. The use of a solenoid results in fewer aberrations, and a cylindrically symmetric focusing of the ions into the focal spot<sup>36,37</sup>. This new FIBIP ion beam optics design uses the same object and focusing distances as used in previous RARAF ion beam designs<sup>33</sup>, thus requiring only minor facility modifications for support of the 7 T magnet. The largest change is the relocation of the limiting aperture from the bottom of the double triplet lens to the two-thirds location in the solenoid. This change greatly increases the acceptance of the solenoid system, allowing for the same particle fluence over larger spot sizes.

**Figure 2A** shows a model of the solenoid focusing system generated using SIMION<sup>®38</sup>, a software for simulations of ion beam trajectories. The magnetic field was constructed using the Poisson SUPERFISH<sup>39</sup> field model and imported into SIMION. Note the aperture at the two-thirds point in the solenoid. The Si<sub>3</sub>N<sub>4</sub> vacuum window is placed  $\approx$ 100  $\mu$ m below the focus point to minimize the distance in air that the ion beam travels before irradiating the sample.

Two apertures are used to define the beam: the object aperture of the focusing system and the limiting aperture defining the beam envelope. The object aperture (Technisches Bernd Fisher, Darmstadt, Germany; also used as the object aperture for our previous microbeam systems<sup>33</sup>) consists of two pairs of precision ground tungsten rod held apart to form a very controlled wedge from 10  $\mu$ m to 150  $\mu$ m. The two pairs are mounted orthogonally to each other and provide semi-rectangular apertures between 10  $\mu$ m and 150  $\mu$ m. The crossed wedges are pictured in **Figure 2B**. The limiting aperture is a precision-machined aperture held by a compressive assembly at the two-thirds point in the solenoid field on a custom mounting system designed and built in our machine shop. The mounting system guarantees alignment with the solenoid and with the Si<sub>3</sub>N<sub>4</sub> exit window. This assembly is shown in a schematic in **Figure 2C**. The limiting aperture is an interchangeable brass disc with center holes ranging from 400  $\mu$ m up to 4 mm depending on the spot size required for the experiment being performed.

The FIBIP ion beam is characterized for size and fluence through our standard dosimetry systems<sup>40-42</sup>. Briefly, the primary beam size measurement is performed using the knife-edge occlusion method for small (<250  $\mu\text{m}$ ) beams<sup>33</sup>. This method uses a sharp edge that is longer than the beam width, stepped through the diameter of the beam while the percentage of the beam passing the edge is measured at each step. This percentage is then plotted out from the 10%-90% positions and linearly fitted to 0% and 100% through those locations for the measured beam diameter. The dosimetry for small beam sizes is through the counting of particles in a solid-state detector for measuring the fluence of the beam in the current beam spot. For larger beam sizes (250  $\mu\text{m}$  to 2 mm) EBT3 Gafchromic<sup>TM</sup> film (Ashland Advanced Materials, Bridgewater, NJ) with an exposed active layer is used for measuring the beam spot size through observation of the darkening of the film. The film darkening is also used as the dosimetry of the beam for a given spot size and observed for uniformity across the whole irradiation spot. For all spot sizes, the beam is controlled in an on/off manner delivering the required fluence for the experimental dose requested.

For all beam sizes and particle types, LET is verified using a tissue equivalent gas proportion counter (TEPC)<sup>41</sup>. The TEPC has been used for more than 40 years as our LET verification system for dosimetry on our Track Segment Facility<sup>41,42</sup>.

### *Cell-culture environmental control*

Our imaging and irradiation geometry requires access to both sides of the sample for simultaneous irradiation and imaging. However, this geometry poses a challenge for standard environmental control methods. To address this challenge, we developed a custom cell-culture environmental control system to ensure constant temperature, stable pH levels, and minimal evaporation of the culture medium during irradiation and imaging (**Figure 3**).

In our design, gas (5% CO<sub>2</sub>; Balance Air) flows over a cell culture after it is pushed through Gibco<sup>TM</sup> Hanks' Buffered Saline Solution in a gas-washing bottle (PYREX<sup>TM</sup> 31770250EC) placed on a hot plate (Scilogex MS-H280-Pro). This setup minimizes disruption to the culture medium as the aluminum shroud covers the petri dish, ensuring constant gas flow (inset in **Figure 1**). The availability of incubators in the RARAF microbeam room and the ability to swiftly move

the shroud in the vertical direction allow the cell culture dish to be positioned for experiments in less than a minute after being removed from the incubator.

To maintain a controlled temperature ( $37\text{ }^{\circ}\text{C} \pm 0.5\text{ }^{\circ}\text{C}$ ) in the cell culture medium for extended periods ( $\geq 2\text{ h}$ ), the aluminum sample holder, aluminum shroud, and the water immersion objective lens (N20X-PFH 20X Olympus) are elevated to  $\approx 40\text{ }^{\circ}\text{C}$ . For the objective lens we used a 2-channel temperature controller (Okolab H401-T-Controller). The shroud and sample holders were heated using a homebuilt system based on Inkbird ITC-106VH PID Temperature Thermostat Controllers, with polyimide thermofoil heater (Minco Inc, Minneapolis, MN) and RTD temperature sensors (Minco).

### *System Integration*

As shown in **Figure 1**, the final integrated system includes the SCAPE microscope mounted above the vertical beam's focal point. SCAPE's primary objective (O1) was mounted on a rotation stage to enable the sample dish to be easily positioned above the ion beam snout. Fine repositioning of the sample was achieved by placing the sample holder on a 3D translation stage assembled using Thorlabs XRP50 stages providing  $10\text{ }\mu\text{m}$  reproducibility. SCAPE's graphical user interface (Matlab™) was modified to enable both fast imaging and time-lapse acquisition, as well as triggering to enable time synchronization with radiation delivery.

## **Results**

### *Using FIBIP/SCAPE to explore 3D tumor model responses to radiation*

The FIBIP integrated system has been tested using a 3D tumor construct model developed at the Center for Radiological Research<sup>43-45</sup>. These models use cell lines injected at known concentrations into a gel matrix where they are incubated for 24-48 h before imaging. The injected cell bolus forms a solid tumor core, and begins branching out into the gel in a similar way to tumor growth and development in an *in vivo* environment. By observing cells in these cultures before, during, and after irradiation we can elucidate the effects of radiation at the cellular level over time.



For this proof-of-principle study, U87 Glioblastoma cells were chosen as an aggressive tumor model type known to grow rapidly in the 3D model systems. 3D cultures were set up as described previously <sup>46</sup>.

For our first example (**Figure 4**), we stained a 3D cell culture with Cyto-Red (Biosettia) and pGreenFire 2.0 NFkB reporter (SBI). Image volumes were acquired with an offline version of SCAPE scanning for 1 s every 60 s for 1.5 h (imaged at  $2 \times 1.17 \times 0.95$  voxels over a volume of  $800 \times 700 \times 380$   $\mu\text{m}$  xyz). Image panels show the motility of cells during this time-lapse acquisition. **Supplemental Movie 1** shows this full dataset, permitting the continuous motility of cells to be appreciated along with the lack of photobleaching throughout the 1.5 h imaging session.

For our second example, we stained a 3D cell culture with CellTracker Red and Oregon Green free calcium reporter (Oregon Green BAPTA-1 AM) 30 min prior to imaging and irradiation. The stain media was replaced with phenol red free growth media for imaging. After staining, 3D culture model was imaged at  $1.4 \mu\text{m} \times 2 \mu\text{m} \times 1.1 \mu\text{m}$  voxels over a volume  $600 \mu\text{m} \times 600 \mu\text{m} \times 400 \mu\text{m}$ . The images were acquired at 1 volume-per-second at 12 s intervals for 10 min before irradiation and for 10 min following irradiation, with the irradiation taking  $\approx 30$  s (3 frames of acquisition) in the middle of the imaging period. It was determined through preliminary trials that this timing was sufficient for observing variation of free calcium signals in the cells and cell structures over the 20 min imaging sequence while observing evidence of irradiation effects. The samples were irradiated with  $9 \pm 1$  Gy of protons at an average LET of  $12 \text{ keV}/\mu\text{m}$  uniformly in a spot size that circumscribed the imaging area (1.1 mm in diameter).

**Figure 5A** shows a 3D rendering of the 3D tumor model growing in the gel matrix shown as a maximum projection from the top and the two orthogonal sides. **Supplemental Movie 2** shows a dynamic rendering of this data. The red CellTracker signal is used to locate the cells for analysis and for analyzing cell motion through the imaging and irradiation time frame. The Oregon green signal shows calcium activity within the cells. **Figure 5B** shows extracted calcium signals plotted over time for specific cells within the culture. It is observed that before irradiation, the free calcium signals in the cells change significantly over time. Following irradiation (after the red bar in **Figure 5B**) the activity, observed as the amount of changes in the free calcium fold changes, lessens and the calcium levels seem to remain at the level they were at during the irradiation.

This result is interpreted to mean that the irradiation has the immediate effect of stopping cellular calcium activity upon receiving the radiation injury. We attribute this calcium activity to the mechanical motion and metabolism associated with the motility and mobility of the cells as they are growing into the matrix<sup>47</sup>.

## **Discussion**

We have developed and demonstrated a versatile radiation platform to deliver micrometer to mm diameter radiation beams with similar dose deposition (FIBIP). This new irradiation platform has been used to irradiate 3D tumor models based on a cancer cell line. The integrated SCAPE microscopy system and environmental control system permits exploration of mechanistic effects of charged particle radiotherapy at the cellular and tissue levels. We demonstrated that this integrated irradiation and imaging system enables observation of immediate radiation effects, in this example, effects on spontaneous calcium signaling in the 3D sample before, during, and after irradiation over extended periods. We also demonstrated SCAPE's ability to capture long term cellular motility within 3D tumor cultures.

## **Acknowledgements**

This work was supported by the National Cancer Institute U01CA236554 and the National Institute of Biomedical Imaging and Bioengineering P41EB002033 as well as National Institute of Neurological Disorders and Stroke BRAIN initiative grants UF1NS10821 and U01NS094296. The content is solely the responsibility of the authors and does not necessarily represent the official views of the NCI, NIBIB and NINDS.

## **Disclosures**

Intellectual property relating to SCAPE microscopy is licensed to Leica Microsystems and Applied Scientific Instrumentation (ASI) and could financially benefit EMCH and CPC.

## **Data availability**

Data presented may be obtained from the authors upon reasonable request.

## Figures

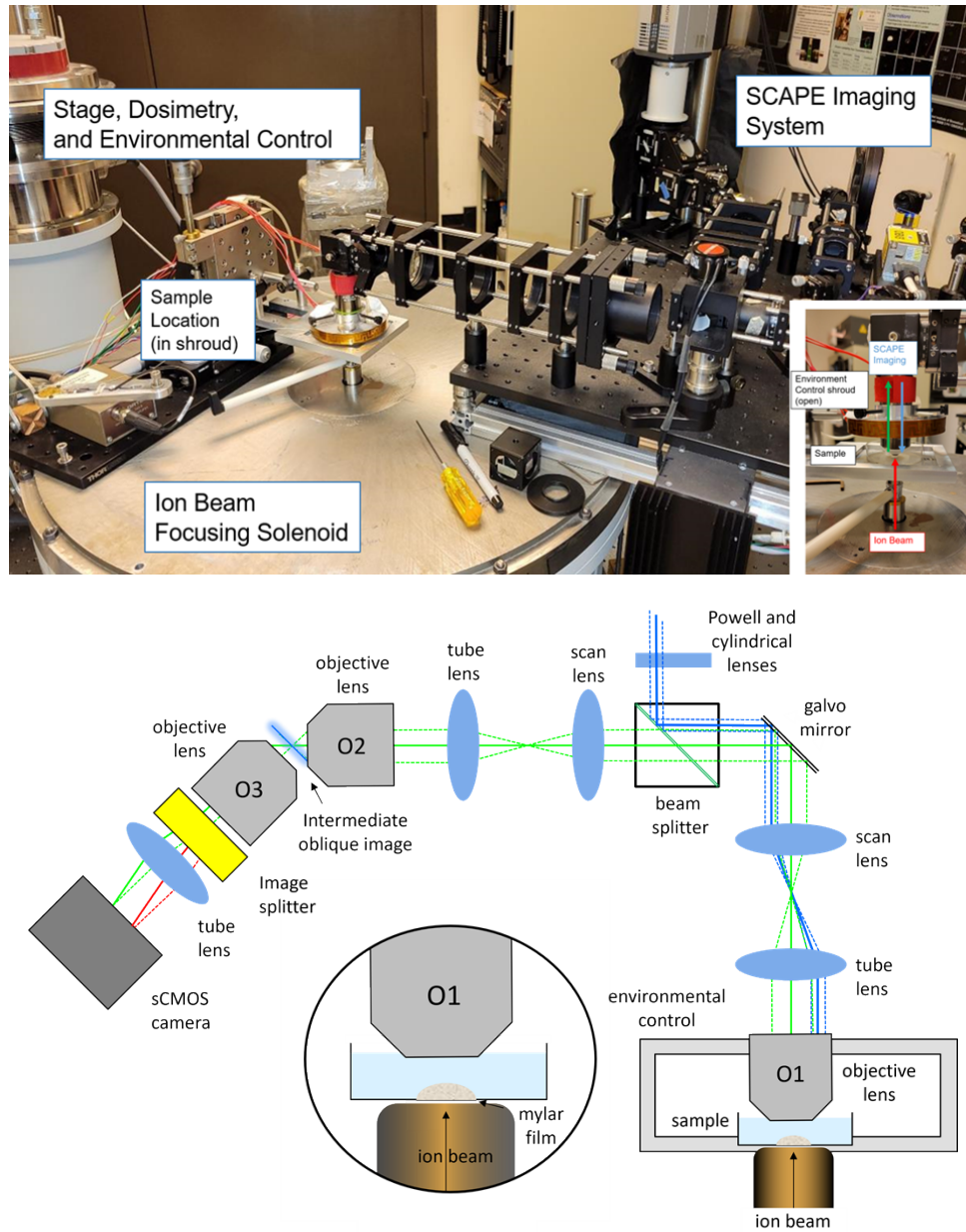


**Figure 1. An integrated system for irradiation and fast 3D microscopy.** Top: Photograph of the RARAF microbeam room with the integrated SCAPE<sup>13</sup> system (to the right) and the cell culture environmental setup (to the left). The inset (bottom right) shows a closer view of the sample holder, cell culture dish, and the shroud around the objective lens. Below: SCAPE optical layout and sample geometry.

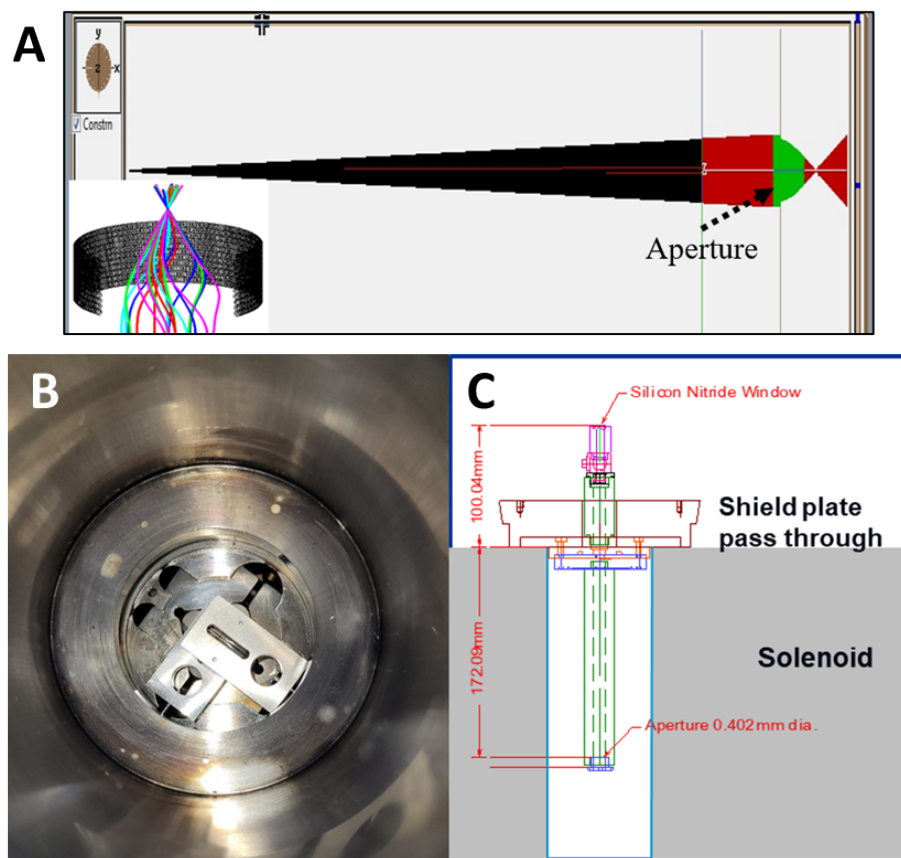


**Figure 2. Expansion and extension of ion beam.** *A:* Simion model of solenoid (green area is solenoid field) focusing of 30 MeV  $C^{6+}$  ions to 2 mm beam spot size. Note the limiting aperture in the green field area. This provides very large beam acceptance for ion fluence effective for irradiation over all our spot sizes. The inset (bottom left) shows trajectories of few particles through the solenoid field. *Bottom:* The object aperture (*B*) and the limiting aperture schematic (*C*) of the FIBIP. The object is a pair of crossed ground tungsten cylinder wedges giving semi rectangular apertures from 10  $\mu m$  to 150  $\mu m$ . The limiting aperture is held at the two-thirds point in the solenoid field and is aligned by construction to the solenoid and the  $Si_3N_4$  window. The limiting aperture is a brass disc held in place by compression with a center hole ranging from 400  $\mu m$  to 4 mm.

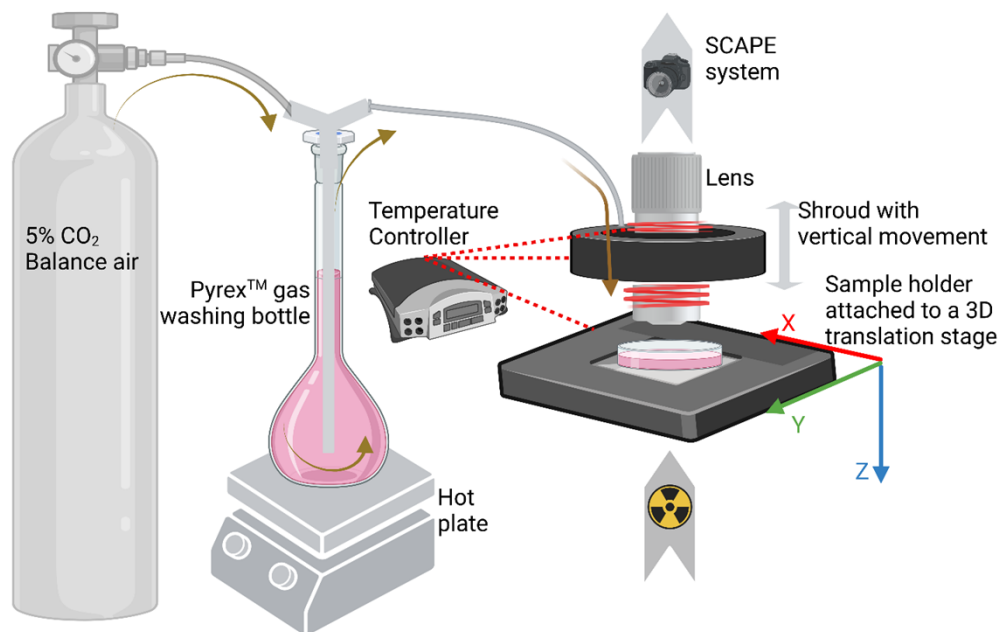


**Figure 3.** *The cell culture environmental scheme* (not drawn to scale) in the RARAF microbeam room for extended ( $\geq 2$  h) imaging and radiation exposures outside an incubator. *Created with BioRender.com*

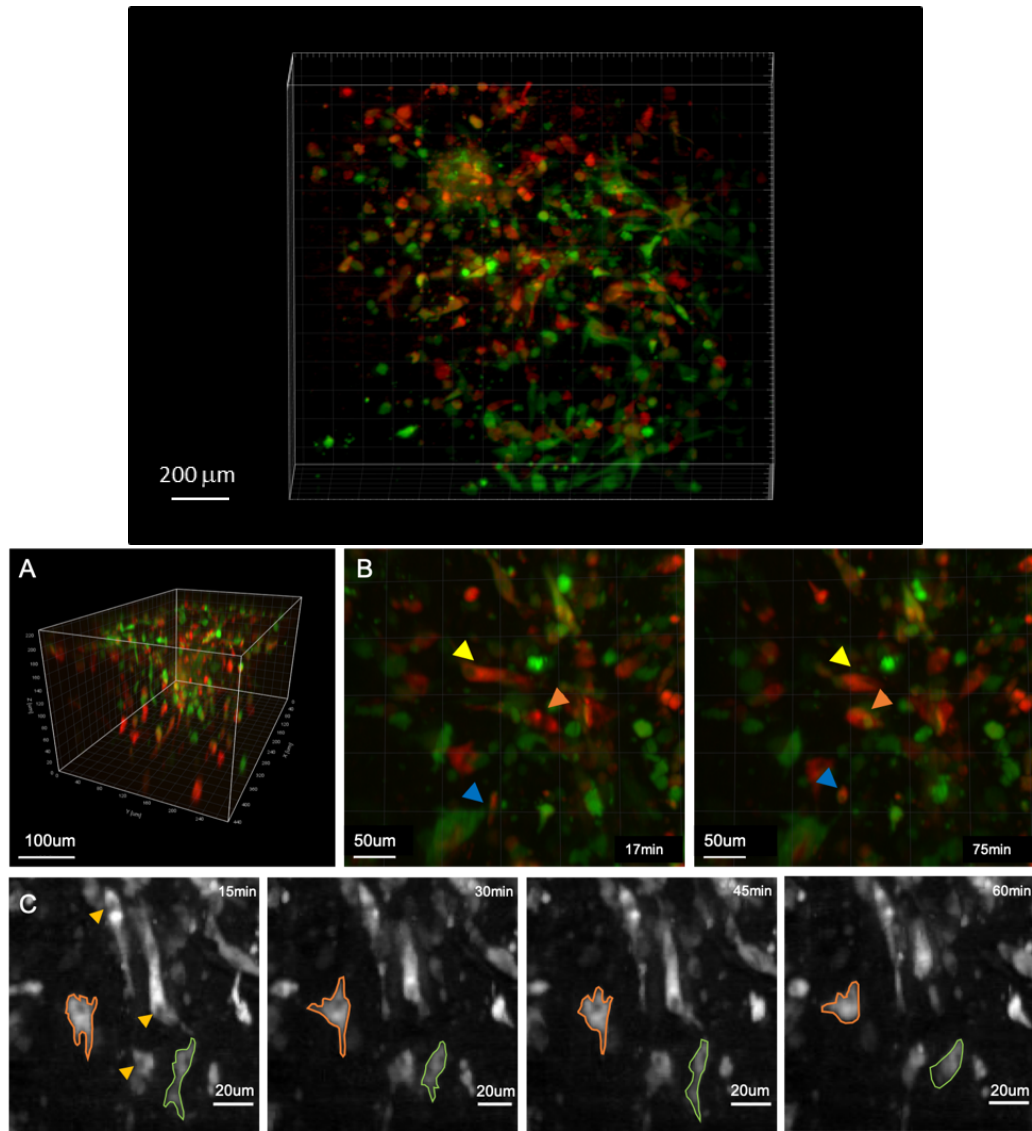


**Figure 4: Examples of cell mobility and motility in 3D U87- glioblastoma culture (without irradiation),** 3D dual color 1.5 h time-lapse acquired using offline SCAPE system. Top: 3D rendering (see **Supplemental Movie 1**). A) Single time point (one 3D volume) of the 1.5 h time lapse acquired. B) Three migrating cells (arrows) shown at two timepoints, 17 min and 75 min. C) Sub-region from A) showing cell deformation and "scouting" behavior over time. Red channel: Cyto-Red (Biosettia), ex 488 nm, em 618/50, Green channel: pGreenFire 2.0 NFkB reporter (SBI), ex 488 nm, em 525/45, laser power 12 mW, acquisition time 2 s per volume every 60 s, total acquisition 1.5 h.

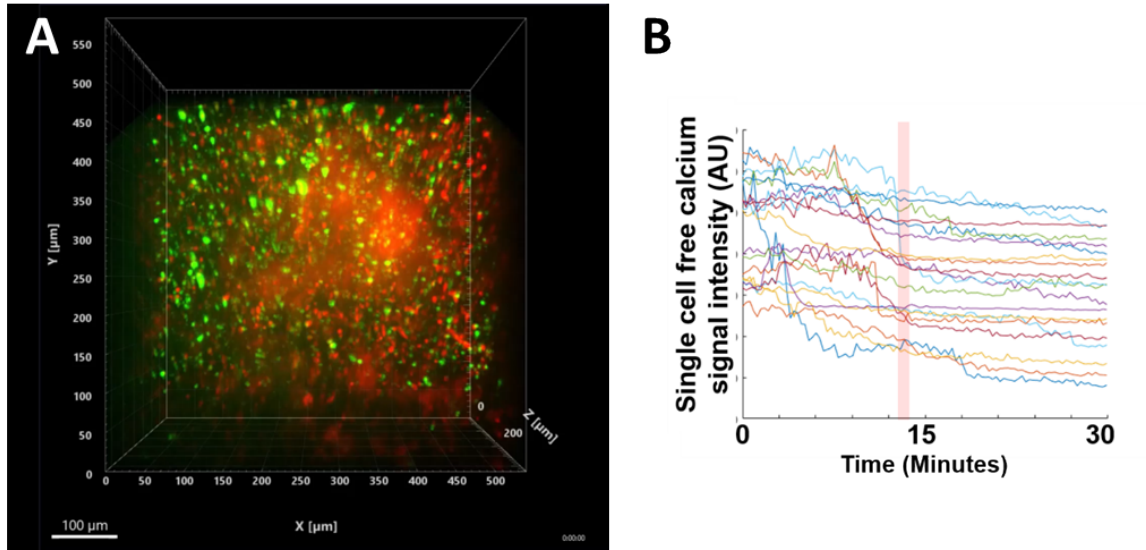
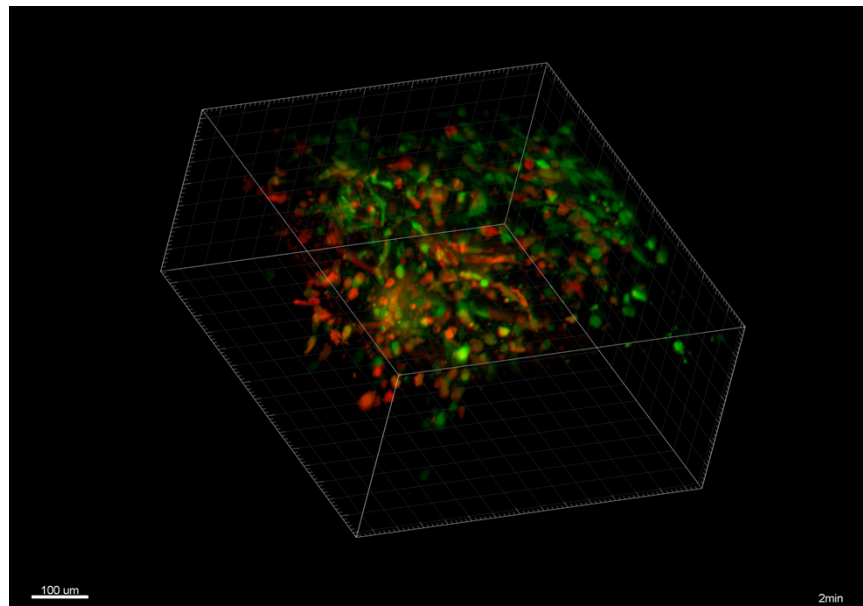


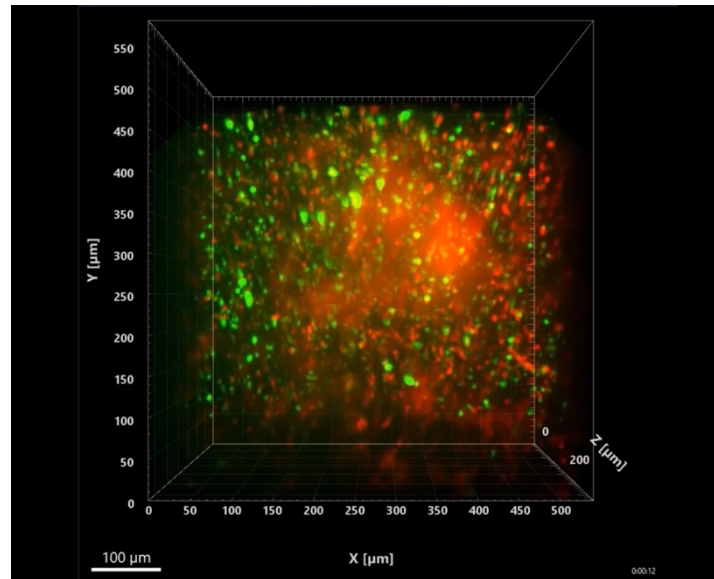
**Figure 5. Intracellular calcium response of U87- glioblastoma culture 3D culture to 9 Gy of protons. A** single frame of a 3D volumetric movie of U87 Glioblastoma cells taken using the SCAPE imaging system on the integrated RARAF FIBIP (left). This volume is  $600\ \mu\text{m} \times 550\ \mu\text{m} \times 300\ \mu\text{m}$  acquired in 1 s. The complete movie is over a span of 30 min with a volume acquired every 12 s. The green label is Oregon Green free calcium reporter and the red label is CellTracker Red membrane label. The calcium signal fold intensity over time for U87 cells exposed to 9 Gy of protons (right). See **Supplemental Movie 2** for dynamic rendering.



## Supplemental Movies



**Supplemental Movie 1.** Dynamic rendering of cell motility SCAPE data shown in Figure 4



**Supplemental Movie 2.** Dynamic rendering of intracellular calcium data during irradiation shown in Figure 5



## References

- 1 Begg, A. C., Stewart, F. A. & Vens, C. Strategies to improve radiotherapy with targeted drugs. *Nature Reviews Cancer* **11**, 239-253 (2011). <https://doi.org:10.1038/nrc3007>
- 2 Delaney, G., Jacob, S., Featherstone, C. & Barton, M. The role of radiotherapy in cancer treatment. *Cancer* **104**, 1129-1137 (2005). <https://doi.org:https://doi.org/10.1002/cncr.21324>
- 3 Illicic, K., Combs, S. E. & Schmid, T. E. New insights in the relative radiobiological effectiveness of proton irradiation. *Radiation Oncology* **13**, 6 (2018). <https://doi.org:10.1186/s13014-018-0954-9>
- 4 Pompos, A., Durante, M. & Choy, H. Heavy Ions in Cancer Therapy. *JAMA Oncology* **2**, 1539-1540 (2016). <https://doi.org:10.1001/jamaoncol.2016.2646>
- 5 Kamada, T. *et al.* Carbon ion radiotherapy in Japan: an assessment of 20 years of clinical experience. *The Lancet. Oncology* **16**, e93-e100 (2015). [https://doi.org:10.1016/S1470-2045\(14\)70412-7](https://doi.org:10.1016/S1470-2045(14)70412-7)
- 6 Matsunaga, A. *et al.* Carbon-ion beam treatment induces systemic antitumor immunity against murine squamous cell carcinoma. *Cancer* **116**, 3740-3748 (2010). <https://doi.org:10.1002/cncr.25134>
- 7 Durante, M., Brenner, D. J. & Formenti, S. C. Does Heavy Ion Therapy Work Through the Immune System? *International journal of radiation oncology, biology, physics* **96**, 934-936 (2016). <https://doi.org:10.1016/j.ijrobp.2016.08.037>
- 8 Mohamad, O., Makishima, H. & Kamada, T. Evolution of Carbon Ion Radiotherapy at the National Institute of Radiological Sciences in Japan. *Cancers* **10** (2018). <https://doi.org:10.3390/cancers10030066>
- 9 Brownstein, J. M. *et al.* Characterizing the Potency and Impact of Carbon Ion Therapy in a Primary Mouse Model of Soft Tissue Sarcoma. *Molecular cancer therapeutics* **17**, 858-868 (2018). <https://doi.org:10.1158/1535-7163.MCT-17-0965>
- 10 Ohkubo, Y. *et al.* Combining carbon ion radiotherapy and local injection of alpha-galactosylceramide-pulsed dendritic cells inhibits lung metastases in an in vivo murine model. *International journal of radiation oncology, biology, physics* **78**, 1524-1531 (2010). <https://doi.org:10.1016/j.ijrobp.2010.06.048>
- 11 Jasper, A. *et al.* Optimization of a GCaMP Calcium Indicator for Neural Activity Imaging. *The Journal of Neuroscience* **32**, 13819 (2012). <https://doi.org:10.1523/JNEUROSCI.2601-12.2012>
- 12 Lazzari, G. *et al.* Light sheet fluorescence microscopy versus confocal microscopy: in quest of a suitable tool to assess drug and nanomedicine penetration into multicellular tumor spheroids. *European Journal of Pharmaceutics and Biopharmaceutics* **142**, 195-203 (2019). <https://doi.org:https://doi.org/10.1016/j.ejpb.2019.06.019>
- 13 Bouchard, M. B. *et al.* Swept confocally-aligned planar excitation (SCAPE) microscopy for high-speed volumetric imaging of behaving organisms. *Nature Photonics* **9**, 113-119 (2015). <https://doi.org:10.1038/nphoton.2014.323>
- 14 Voleti, V. *et al.* Real-time volumetric microscopy of in vivo dynamics and large-scale samples with SCAPE 2.0. *Nature Methods* **16**, 1054-1062 (2019). <https://doi.org:10.1038/s41592-019-0579-4>
- 15 England, M. J. *et al.* Automated microbeam observation environment for biological analysis—Custom portable environmental control applied to a vertical microbeam system. *Sensors and Actuators B: Chemical* **239**, 1134-1143 (2017). <https://doi.org:https://doi.org/10.1016/j.snb.2016.08.076>
- 16 Hillman, E. M. C. *et al.* High-speed 3D imaging of cellular activity in the brain using axially-extended beams and light sheets. *Current Opinion in Neurobiology* **50**, 190-200 (2018). <https://doi.org:https://doi.org/10.1016/j.conb.2018.03.007>

- 17 Randers-Pehrson, G. Microbeams, microdosimetry and specific dose. *Radiation protection dosimetry* **99**, 471-472 (2002).
- 18 Marino, S. A. 50 Years of the Radiological Research Accelerator Facility (RARAF). *Radiation Research* **187**, 413-423, 411 (2017).
- 19 Griffith, L. G. & Swartz, M. A. Capturing complex 3D tissue physiology in vitro. *Nature Reviews Molecular Cell Biology* **7**, 211-224 (2006). <https://doi.org:10.1038/nrm1858>
- 20 Durante, M. & Friedl, A. A. New challenges in radiobiology research with microbeams. *Radiation and Environmental Biophysics* **50**, 335-338 (2011). <https://doi.org:10.1007/s00411-011-0373-x>
- 21 Coutu, D. L. & Schroeder, T. Probing cellular processes by long-term live imaging – historic problems and current solutions. *Journal of Cell Science* **126**, 3805-3815 (2013). <https://doi.org:10.1242/jcs.118349>
- 22 Dunsby, C. Optically sectioned imaging by oblique plane microscopy. *Opt. Express* **16**, 20306-20316 (2008). <https://doi.org:10.1364/OE.16.020306>
- 23 Bigelow, A. W. *et al.* Ion, X-Ray, UV And Neutron Microbeam Systems For Cell Irradiation. *AIP Conference Proceedings* **1336**, 351-355 (2011).
- 24 Dymnikov, A. D., Brenner, D. J., Johnson, G. & Randers-Pehrson, G. Theoretical study of short electrostatic lens for the Columbia ion microprobe. *Rev. Sci. Instrum.* **71**, 1646-1650 (2000). <https://doi.org:10.1063/1.1150512>
- 25 Garty, G. *et al.* Design of a novel flow-and-shoot microbeam. *Radiation protection dosimetry* **143**, 344-348 (2011). <https://doi.org:10.1093/rpd/ncq476>
- 26 Garty, G., Ross, G. J., Bigelow, A. W., Randers-Pehrson, G. & Brenner, D. J. Testing the stand-alone microbeam at Columbia University. *Radiation protection dosimetry* **122**, 292-296 (2006). <https://doi.org:ncl454> [pii] 10.1093/rpd/ncl454
- 27 Grad, M., Bigelow, A. W., Garty, G., Attinger, D. & Brenner, D. J. Optofluidic cell manipulation for a biological microbeam. *The Review of Scientific Instruments* **84**, 014301 (2013). <https://doi.org:10.1063/1.4774043>
- 28 Grad, M., Harken, A., Randers-Pehrson, G., Attinger, D. & Brenner, D. An ultra-thin Schottky diode as a transmission particle detector for biological microbeams. *Journal of Instrumentation* **7**, P12001 (2012).
- 29 Harken, A. D., Randers-Pehrson, G., Johnson, G. W. & Brenner, D. J. The Columbia University proton-induced soft x-ray microbeam. *Nuclear instruments & methods in physics research. Section B, Beam interactions with materials and atoms* **269**, 1992-1996 (2011). <https://doi.org:10.1016/j.nimb.2011.05.033>
- 30 Miller, R. C. *et al.* The Biological Effectiveness of Radon-Progeny Alpha Particles. II. Oncogenic Transformation as a Function of Linear Energy Transfer. *Radiation Research* **142**, 54-60 (1995). <https://doi.org:10.2307/3578966>
- 31 Ponnaiya, B., Jenkins-Baker, G., Randers-Pehrson, G. & Geard, C. R. Quantifying a bystander response following microbeam irradiation using single-cell RT-PCR analyses. *Exp Hematol* **35**, 64-68 (2007). [https://doi.org:S0301-472X\(07\)00016-1](https://doi.org:S0301-472X(07)00016-1) [pii] 10.1016/j.exphem.2007.01.013
- 32 Randers-Pehrson, G., Geard, C. R., Johnson, G., Elliston, C. D. & Brenner, D. J. The Columbia University single-ion microbeam. *Radiation Research* **156**, 210-214 (2001). [https://doi.org:10.1667/0033-7587\(2001\)156\[0210:tcusim\]2.0.co;2](https://doi.org:10.1667/0033-7587(2001)156[0210:tcusim]2.0.co;2)
- 33 Randers-Pehrson, G. *et al.* The Columbia University sub-micron charged particle beam. *Nuclear Instruments & Methods in Physics Research Section B: Beam Interactions with Materials and Atoms* **609**, 294-299 (2009). <https://doi.org:10.1016/j.nima.2009.08.041>
- 34 Vasquez, M. *et al.* in *Proceedings of the 14th International Congress of Radiation Research (ICRR)* 77 (Warsaw, Poland, 2011).

- 35 Xu, Y. *et al.* An accelerator-based neutron microbeam system for studies of radiation effects. *Radiation protection dosimetry* **145**, 373-376 (2011). <https://doi.org:10.1093/rpd/ncq424>
- 36 Matsuda, H. & Wollnik, H. Third order transfer matrices for the fringing field of magnetic and electrostatic quadrupole lenses. *Nuclear Instruments and Methods* **103**, 117-124 (1972). [https://doi.org:10.1016/0029-554x\(72\)90468-5](https://doi.org:10.1016/0029-554x(72)90468-5)
- 37 Wollnik, H., Yavor, M. I. & Kalimov, A. G. Low aberration focusing system for a proton nanoprobe. *Rev. Sci. Instrum.* **69**, 4116-4119 (1998).
- 38 Dahl, D. A. simion for the personal computer in reflection. *Int J Mass Spec* **200**, 3-25 (2000). [https://doi.org:http://dx.doi.org/10.1016/S1387-3806\(00\)00305-5](https://doi.org:http://dx.doi.org/10.1016/S1387-3806(00)00305-5)
- 39 Billen, J. H. & Young, L. M. in *Proceedings of the 1993 Particle Accelerator Conference* 790-792 vol.792 (1993).
- 40 Garty, G. *et al.* Ultra-high dose rate FLASH irradiator at the radiological research accelerator facility. *Scientific reports* **12**, 22149 (2022). <https://doi.org:10.1038/s41598-022-19211-7>
- 41 Garty, G., Harken, A. D. & Brenner, D. J. Traceable dosimetry for MeV ion beams. *Journal of instrumentation : an IOP and SISSA journal* **17** (2022). <https://doi.org:10.1088/1748-0221/17/02/t02002>
- 42 Bird, R. P., Rohrig, N., Colvett, R. D., Geard, C. R. & Marino, S. A. Inactivation of Synchronized Chinese Hamster V79 Cells with Charged-Particle Track Segments. *Radiation Research* **82**, 277-289 (1980). <https://doi.org:10.2307/3575379>
- 43 Grabham, P., Hu, B., Sharma, P. & Geard, C. Effects of ionizing radiation on three-dimensional human vessel models: differential effects according to radiation quality and cellular development. *Radiation Research* **175**, 21-28 (2011). <https://doi.org:10.1667/RR2289.1> [pii] 10.1667/RR2289.1
- 44 Grabham, P. & Sharma, P. The effects of radiation on angiogenesis. *Vascular cell* **5**, 19 (2013). <https://doi.org:10.1186/2045-824x-5-19>
- 45 Grabham, P., Sharma, P., Bigelow, A. & Geard, C. Two distinct types of the inhibition of vasculogenesis by different species of charged particles. *Vascular cell* **5**, 16 (2013). <https://doi.org:10.1186/2045-824x-5-16>
- 46 Xue, G. *et al.* Reprogramming mediated radio-resistance of 3D-grown cancer cells. *Journal of radiation research* **56**, 656-662 (2015). <https://doi.org:10.1093/jrr/rrv018>
- 47 Goldberg, D. J. & Grabham, P. W. Braking news: calcium in the growth cone. *Neuron* **22**, 423-425 (1999). [https://doi.org:10.1016/s0896-6273\(00\)80697-2](https://doi.org:10.1016/s0896-6273(00)80697-2)